Force Control in One Legged Hopping Robot while Landing

V. L. Krishnan, P. M. Pathak*, S. C. Jain

Indian Institute of Technology, Roorkee, India, 247667

*Corresponding author (email: pushpfme@iitr.ernet.in)

Abstract

In this paper, the issue of control of impact forces generated during the interaction between the hopping robot toe and the ground during landing has been considered. The force thus generated can damage the robot altogether. With the objective to control these impact forces impedance control strategy has been applied to the hopping robot system. The dynamics pertaining to the impact between robot toe and ground has been modeled as in case of a ball bouncing on the ground. Bond Graph theory has been used for the modeling of the hopping robot system. Simulation results show that impact forces generated during the landing has been controlled to a specified limiting value. This model and the corresponding analysis can be further extended for understanding the dynamics involved in continuous hopping of robot with constant height and velocity control.

Keywords: Hopping robot, Impact forces, Impedance control

1 Introduction

In recent years, legged robots, especially biped robots, have been developed to the extent that human-like walking has become possible. In the next stage, robots need to move faster and get over larger obstacles. In this respect, hopping robots offers a potential solution. Due to the possibility of adjusting the stride length irrespective of the structural limits of a hopping robot, it can move faster and avoid larger obstacles than walking. Hopping robots can move with greater dexterity in an environment characterized by holes, steps and bumps. But an important issue related to hopping robot locomotion is reducing the impact force from the ground at the instant of robot landing which may, otherwise, cause damage to robot.

In order to resolve this problem, Raibert [1] used hydraulic cylinders and Hyon *et al.* [2] used mechanical springs in their robotic legs. However, Hydraulic cylinders don't have enough control performance, especially in the edge of the cylinders. Considering hopping as an extended function of walking, use of mechanical springs makes the hopping robot highly dependent on spring characteristics and the control to be complicated. Hence, suppressing impact force in the landing phase without cylinders or mechanical springs is a big issue to be dealt with. In addition to the force control during landing, it is also important to achieve a desired position of center of gravity (CG) of the

hopping robot at the bottom most point i.e. bottom of stance phase. This ensures good trajectory robustness during the next hop.

In order to deal with these issues, Sato *et al.* [3] has used a combined method of soft landing trajectory of robot body and optimal approach velocity to the ground. Fujii and Ohnishi [4] investigated this issue further and proposed a smooth transition method from compliance control to position control. However these methods could not achieve the desired objective of constant force control during the landing phase and precise position control at the bottom.

In this paper the issue under consideration is dealt with by controlling the driving point stiffness (impedance) at the interaction port between hopping robot toe and the physical ground i.e. environment. Pathak *et al.* [5] have used this control strategy employing passive degree of freedom (DOF) in controller domain for the control of interaction forces between space robot tip and environment. The proposed controller deals adequately with the issue of force (compliance) control i.e. reducing ground impact forces at touchdown and position control at bottom so as to prepare hopping robot for the next hop. Bond Graph theory [6] has been used for the modeling of the hopping robot system. Simulations have been performed using SYMBOLS Shakti [7], bond graph modeling software.

The paper is organized as follows. Section 2 presents the modeling of the impact of hopping robot toe with ground as in case of a ball bouncing on ground. Section 3 presents the dynamic modeling of a hopping robot. Section 4 describes the impedance control scheme being used to control the hopping robot and presents the corresponding simulation results. Section 5 discusses the results and proposes the future work.

2 Modeling of Impact between Hopping Robot Toe and Ground

This section presents the modeling of impact dynamics of a hopping robot toe with ground. The modeling of the phenomenon is inspired from the dynamics of a ball hitting the ground [8]. Fig. 1 shows a schematic figure representing the impact of a ball with ground. The Y-axis of the absolute (inertial) reference frame {A} shown in the figure represents the direction of vertical motion of the ball. In Fig. 1, y_B and y_G represents the displacement of ball and ground with respect to the frame {A}. Similarly, V_B and V_G denote the velocities of the ball and the ground respectively with respect to the inertial reference frame.
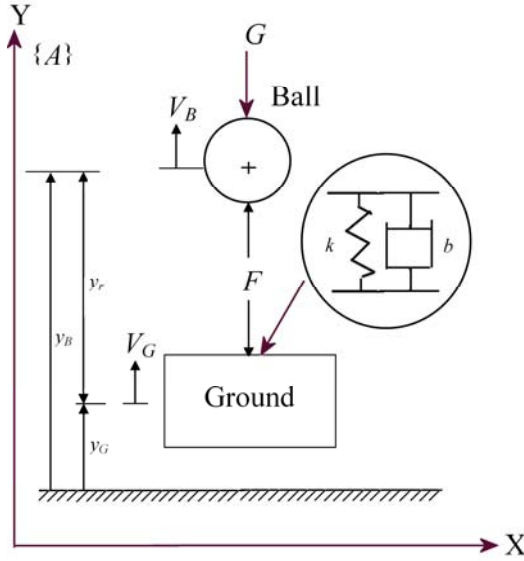
Fig. 1: Schematic diagram representing impact between ball and ground

The velocity of the ball and the ground can be derived by considering their kinematics relationships as:

$$V_B = dy_B / dt \,, \tag{1}$$

$$V_G = dy_G / dt \,. \tag{2}$$

Hence V_r, relative velocity of ball with respect to the ground can be written as,

$$V_r = V_B - V_g \tag{3}$$

Hence, 'y_r' relative displacement of the ball with respect to ground or specifically the point of contact is represented as,

$$y_r = y_0 + \int_0^t (V_B - V_G)d\tau \,. \tag{4}$$

The general system equation for the contact between ground and ball is given by:

$$m\frac{dV_B}{dt} = -mg + F \,, \tag{5}$$

$$b\frac{dy_G}{dt} + ky_G = -F \,, \tag{6}$$

where b is the damping coefficient and k is the spring constant used to model impact between the ball and the ground through spring-damper model. F is the Ground Impact Force generated due to ball-ground interaction and can be evaluated using Eq. (6). Modeling impact between two contact surfaces through spring-damper model is categorized as continuous contact dynamics modeling. In this modeling the normal contact force between the contact surfaces is an explicit function of local indentation δ and its rate [9]. In the case of ball-ground interaction the ground impact force F is a function of y_r. If $y_r > 0$ it implies there is no indentation on either the ground or ball and hence F is equal to zero. The ball will be performing bal-

listic motion under such a situation. The existence or non-existence of the effect of ground-ball contact on the ground impact force can be expressed through Eq. (7) and (8). These equations represent switching of values of parameters b and k between zero and certain finite values.

$$b = b * swi(0, y_r) \,, \tag{7}$$

$$k = k * swi(0, y_r) \,, \tag{8}$$

where swi defines a function such as $swi(0, y_r) = 1$, for $0 \ge y_r$, and $swi(0, y_r) = 0$, for $0 < y_r$.

Hence when $y_r > 0$ i.e. ball is not in contact with the ground, from Eq. (7) and (8) we get $b = k = 0$. Hence, ground impact force F is equal to zero. Substituting $F = 0$ in Eq. (5) and (6), we get $m\dfrac{d^2y_B}{dt^2} = -mg$. $\tag{9}$

When the ball hits the ground, $y_r = 0$. From that moment, the ball and the ground move as if a single system. The system equation governing the ball-ground system during contact phase is obtained by combining Eq. (5) and (6) and is expressed as,

$$m\frac{d^2y_G}{dt^2} + b\frac{dy_G}{dt} + ky_G = -mg \tag{10}$$

The motion of the ball and ground together as a single system consists of two phases. In the first phase the spring compresses until the ball velocity drops to zero. In the second phase, the spring expands during which the ball starts rebounding. During the entire contact phase the relative displacement of the body with the ground is equal to or less than zero and the detachment occurs when it is positive again.

The bond graph implementation of the impact dynamics between the ball and the ground is shown in Fig. 2. Here it is assumed that the ground has zero velocity. Hence the ground velocity junction does not appear in the bond graph in fig. 2.
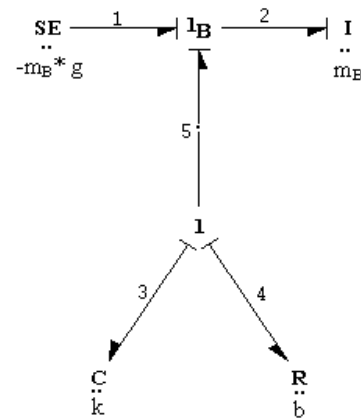
Fig. 2 Bond Graph representing Impact dynamics between Ball and ground

(a)

(b)

(c)
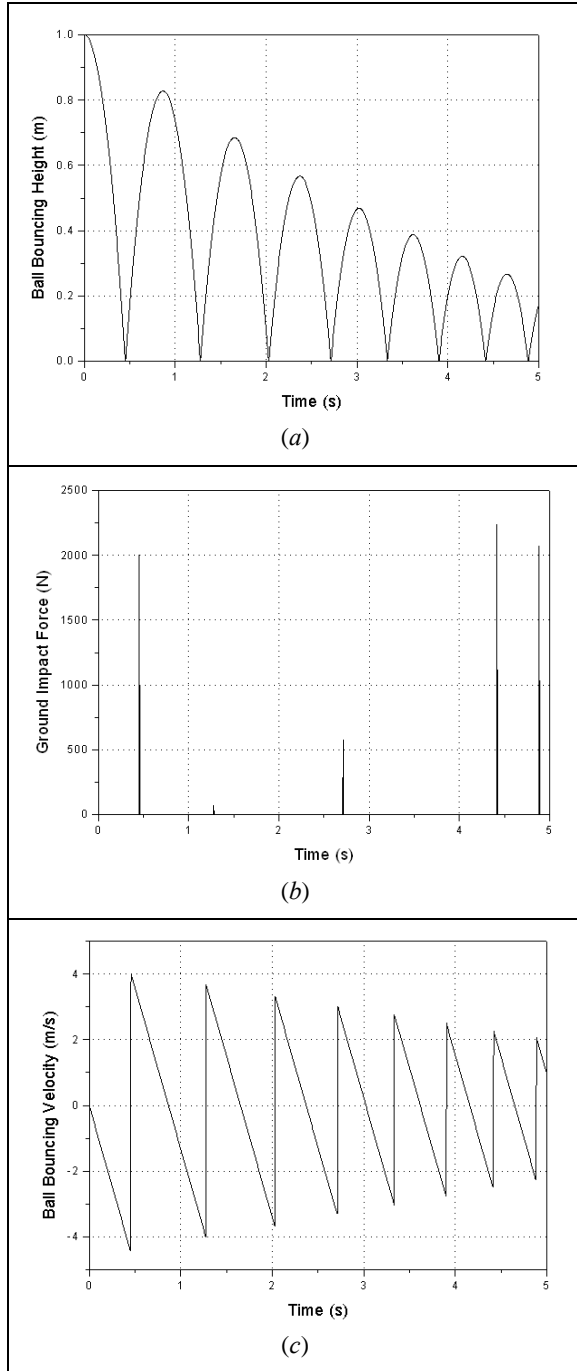
Fig. 3(*a*) Ball Bouncing height (*b*) Ground Impact Force (*c*) Ball Bouncing Velocity

The parameters used for the simulation are m_B = 1.0 kg, spring stiffness (k) = 10^6 N-m, damping coefficient (b) = 60N-s/m, Initial height of the ball above the ground (h) = 1.0m. The corresponding simulation results are represented in Fig. 3. It can be noted from Fig. 3(*a*) that the bouncing height over the consecutive hops decays continuously. Fig. 3(*b*) shows the development of contact forces when ball comes in contact with ground. It should be noted that as since the ground impact force model is based on a linear spring damper system the forces are generated whenever there is an indentation/penetration of the

contact surfaces. Fig. 3(*c*) shows the bouncing ball velocity which decays as time increases. It can be noted from the figure that there is a change in momentum before and after each successive impact.

Thus the ball bouncing over ground furnishes a simple model of impact between two bodies. It is used in the next section for the modeling of impact of a hopping robot toe with the ground.

3 Dynamic Modeling of a Hopping Robot

The hopping robot is modeled as a two mass system based on work carried out by Sato *et al.* [3]. The first mass is body and the second mass is assumed to be concentrated at its leg tip (toe). The two mass points are connected by a linear motor. A schematic of the hopping robot is shown in Fig. 4. The impact dynamics between the robot toe and the ground is modeled on the basis of work presented in the previous section on ball bouncing on the ground. Fig. 5 shows the bond graph of the hopping robot including the representation of robot toe-ground interaction.

The equations of motion of the hopping robot are given as:

$$m_b \, ^A\ddot{z}_b = -F_m - m_b g \tag{11}$$

$$m_t \, ^A\ddot{z}_t = F_m + F_{env} - m_t g \tag{12}$$

Here m_b is the mass of the body; m_t is the mass of the toe, {A} represents the absolute frame which is located at the ground. F_m is the force generated by a linear motor. The ground is modeled as spring-damper. F_{env} is the reaction force from the environment (ground). K_g and R_g are spring constant and damping coefficient of the ground respectively.
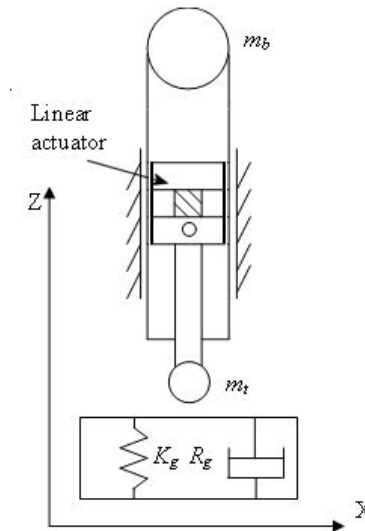
Fig. 4 Schematic diagram of a one-legged hopping robot

The phases and events of a typical hopping cycle are presented in the Table 1. The system parameters are listed in Table 2.

216
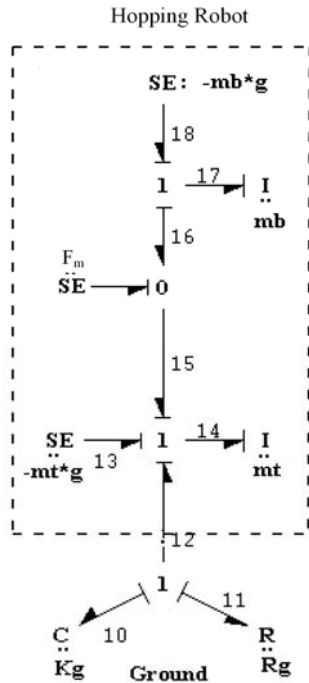
Fig.5. Bond graph model of interaction of a one legged hopping robot with the ground

Table 1: Hopping Cycle

Event	
Top	Body CG is highest
Touchdown	Leg Tip touches ground
Bottom	Body CG is lowest
Liftoff	Leg Tip leaves ground
Phase	
Stance	From touchdown to liftoff
Landing	From touchdown to bottom
Thrusting	From bottom to liftoff
Aerial	From liftoff to touchdown

Table 2: Hopping Robot Parameters

Parameters	Symbol	Value
Body mass	m_b	1.3kg
Leg Mass	m_t	1.0kg
Spring coefficient used to model impact between the leg tip and the ground	K_g	5000N/m
Damping coefficient used to model impact between the leg tip and the ground	R_g	10N-s/m
Body Length	L_b	0.5m

In the next section, an impedance controller is designed along with the hopping robot system to attain the desired control of impact forces.

4 Impedance Control of the Hopping Robot

The impedance of a system at an interaction port is def ined as the ratio between the output effort and the input flow. For applications, demanding a robotic controller to achieve balance between the two characteristics viz. robust trajectory tracking and accommodation of environmental disturbances, the impedance control strategy [6] is best suited.

The impedance control strategy, with regard to the problem under consideration, is based on the body motion compensation. The body motion compensation is so designed that the hopping robot impedance can be modulated to limit the forces of interaction between hopping robot toe and ground. The control paradigm establishes a proper relation between the trajectory controller and the force controller through the manipulation of the impedance. The robot stiffness is made very high during trajectory control, and appropriately modulated during force control. Fig. 6 shows the bond graph model of hopping robot with impedance controller.

In this figure f_{ref} is the reference velocity command for the toe of hopping robot. To incorporate the hopping robot body disturbances in the inertial coordinates, the body velocity is sensed and feedback to the controller.
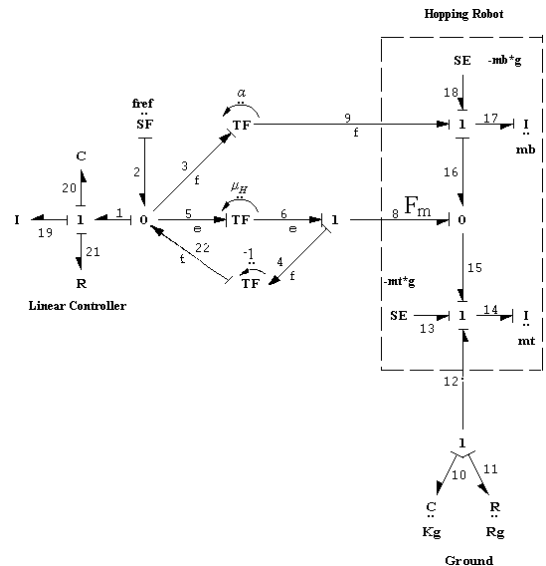
Fig. 6: Bond graph of hopping robot with impedance controller

A gain of α shows the feedback compensation. μ_H represents an effort amplifier. The transfer function between the output flow $F_t(s)$ (i.e., the toe velocity) and the input effort $E_{env}(s)$ (force input from the ground to the toe) represents the admittance $Y_{rob}(s)$ of the robotic system at the interaction port. The impedance $Z_{rob}(s)$ is the inverse of the admittance. Admittance at the interaction port can be

determined from the bond graph shown in Fig. 6. The body and toe weights are not considered in this analysis as they can be treated separately as the disturbance force. Now, applying the constitutive law at junction '1' corresponding to robot toe, we obtain

$$e_{12}(t) = e_{14}(t) - e_{15}(t) ,$$

Taking Laplace transform on both sides of above expression, we obtain

$$E_{12}(s) = E_{14}(s) - E_{15}(s) , \tag{13}$$

$$e_{14}(t) = m_t \frac{d}{dt} f_{14}(t) , \tag{14}$$

Where, e (t) and f (t) are respectively the effort (generalized force) and flow (generalized velocity) variables associated with corresponding bonds of Bond Graph. Taking Laplace transform on both sides of Eq. (14) yields,

$$E_{14}(s) = M_t s F_{14}(s) = \frac{F_{14}(s)}{P_t(s)} . \tag{15}$$

From the bond graph, using constituent laws of junctions it can be obtained that

$$E_{15}(s) = \mu_H E_1(s) , \tag{16}$$

Where, μ_H is the high feed-forward gain. Constitutive law at junction '1', corresponding to the controller is given by:

$$e_1(t) = e_{19}(t) + e_{20}(t) + e_{21}(t) .$$

Taking Laplace transform on both sides, we get

$$C(s) = \frac{E_1(s)}{F_1(s)} = \frac{(M_c s^2 + R_c s + K_c)}{s} . \tag{17}$$

Where, M_c, R_c and K_c are respectively the inertia (differential gain), resistance (proportional gain) and stiffness (integral gain) of the controller. Substituting $E_1(s)$ from Equation (17) into Equation (16), we obtain

$$E_{15}(s) = \mu_H F_1(s) C(s) . \tag{18}$$

Next $F_1(s)$ can be determined by writing the constituent law at junction '0' (one which is supplying flow input to controller):

$$f_1(t) - f_2(t) + f_3(t) + f_{22}(t) = 0 ,$$

$$f_1(t) = -[f_3(t) + f_{22}(t)] . \tag{19}$$

Transfer function is evaluated without considering the reference trajectory. Applying constitutive laws at various junctions, we obtain

$$f_3(t) = \alpha f_{17}(t) = \alpha f_b(t) , \tag{20}$$

Where, $f_b(t)$ is the body velocity or flow variable associated with the body mass point and α is body compensation gain (flow feedback gain)

$$f_{22}(t) = f_8(t) = f_{14}(t) - f_{17}(t) = f_t(t) - f_b(t) . \tag{21}$$

Now substituting $f_3(t)$ and $f_{22}(t)$ respectively from Eq. (20) and Eq. (21) into Eq. (19)

$$f_1(t) = -[f_3(t) + f_{22}(t)] = -[\alpha f_{17}(t) + f_{14}(t) - f_{17}(t)] ,$$

$$f_1(t) = [(1-\alpha) f_{17}(t) - f_{14}(t)] . \tag{22}$$

Taking Laplace transform on both sides of Eq. (22), we get

$$F_1(s) = [(1-\alpha) F_{17}(s) - F_{14}(s)] . \tag{23}$$

Substituting $F_1(s)$ from Eq. (23) into Eq. (18)

$$E_{15}(s) = \mu_H C(s)[(1-\alpha) F_{17}(s) - F_{14}(s)] . \tag{24}$$

Now, $F_{17}(s)$ can be expressed through the transfer function of the robot body $P_b(s)$ as

$$F_{17}(s) = P_b(s) E_{17}(s) . \tag{25}$$

Applying constitutive law at Junction '0' (correspondding to motor torque F$_m$) and at Junction '1' (corresponding to robot toe), we obtain

$$E_{17}(s) = -E_{15}(s) = E_{12}(s) - E_{14}(s) . \tag{26}$$

Substituting E$_{17}$(s) from Eq. (26) in Eq. (25), we get

$$F_{17}(s) = P_b(s)[E_{12}(s) - E_{14}(s)] . \tag{27}$$

Combining Eq. (13), Eq. (15), Eq. (24) and Eq. (27), we obtain

$$E_{12}(s) = \frac{F_{14}(s)}{P_t(s)} - \mu_H C(s)[(1-\alpha) F_{17}(s) - F_{14}(s)] ,$$

$$E_{12}(s) = \frac{F_{14}(s)}{P_t(s)} - \mu_H C(s)$$

$$\left[P_b(s)(1-\alpha) \left[E_{12}(s) - \frac{F_{14}(s)}{P_t(s)} \right] - F_{14}(s) \right] . \tag{28}$$

Simplifying the above equation we get,

$$E_{12}(s)[1 + \mu_H C(s)(1-\alpha) P_b(s)]$$

$$= F_{14}(s) \left[\frac{1}{P_t(s)} + \mu_H C(s) + \mu_H C(s)(1-\alpha) \left[\frac{P_b(s)}{P_t(s)} \right] \right] .$$

As since Admittance at the interaction port between hopping robot toe and ground is defined as,

$$Y_{rob}(s) = \frac{1}{Z_{rob}(s)} = \frac{F_t(s)}{E_{env}(s)} = \frac{F_{14}(s)}{E_{12}(s)}$$

Admittance or impedance at the interaction port is represented as

$$Y_{rob}(s) = \frac{P_t(s)[1 + \mu_H C(s)(1-\alpha) P_b(s)]}{[1 + \mu_H C(s) P_t(s) + \mu_H C(s)(1-\alpha) P_b(s)]} . \tag{29}$$

Eq. (29) indicates two distinct behavior of the system.

1. When $\alpha = 1$, and $\mu_H \gg 1$, $Y_{rob}(s) = 1/Z_{rob}(s) = 1/(\mu_H C(s))$, i.e., toe trajectory is not disturbed by either toe or body inertia so toe can follow the commanded trajectory.

2. When $\alpha < 1$, modulation of the impedance to accommodate the interaction forces is possible.

The heuristic expression for modulation of α is given by,

$$\alpha = 1 - swi(F(t), F_{\lim})$$

$$\left[K_{ini} + K_{GP}(F(t) - F_{\lim}) + K_{GI} \int (F(t) - F_{\lim}) dt \right] \tag{30}$$

where $F(t)$ is the actual contact force obtained from force sensor; F_{lim} is the limiting value of the force specified, K_{ini} is a constant (a bias), K_{GP} is a proportional gain term, and K_{GI} is an integral gain term. Eq. (30) represents a proportional-integral control. The *swi* defines a function such as $swi(a,b)=1$, for $a \geq b$, and $swi(a,b)=0$, for $a < b$, where a, b are variable.

The bond graph implementation of the impedance controller with the hopping robot system is shown in Fig. 6. Simulation is carried out using SYMBOLS Shakti software. The reference trajectory to be followed by robot toe

is taken as a half rectified sine trajectory of amplitude 2A, and is given by Eq. (31) as

$$y = 2A * \sin(2\pi t + \pi) * swi[\sin(2\pi t + \pi), 0]. \quad (31)$$

Then the reference velocity command for the toe, is given by,

$$\dot{y} = 4A\pi \cos(2\pi t + \pi) * swi[\sin(2\pi t + \pi), 0], \quad (32)$$

Table 3: Controller parameters

Parameters	Symbol	Value
Effort amplifier gain	μ_H	4
Controller Proportional gain	r_c	10
Controller Derivative gain	m_c	1
Controller Integral gain	K_c	500
Limiting Force	F_{lim}	30 N
Gain (Initial Biasing)	K_{ini}	0.00
Proportional Gain	K_{GP}	0.001
Integral Gain	K_{GI}	0.001

At the start of simulation the tip trajectory is initialized to reference trajectory to reduce the initial errors. The parameters values used in simulation are given in Table 2 and Table 3.
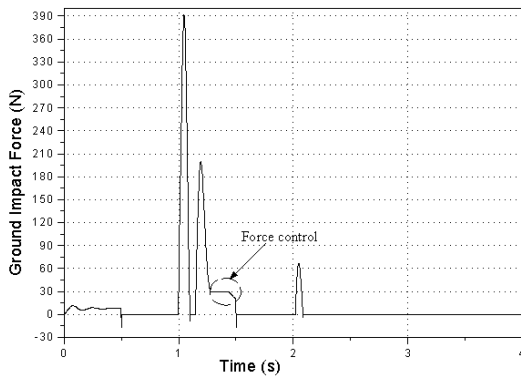
(a)
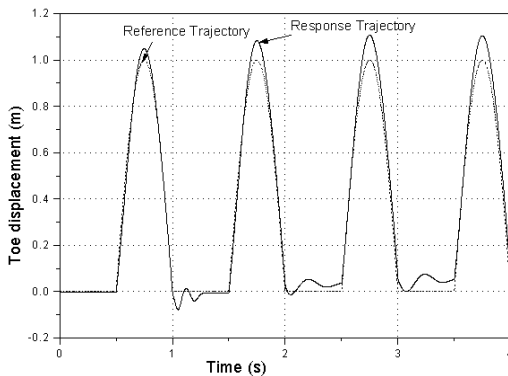
(b)

Fig. 7(a) Ground Impact Force (b) Toe vertical displacement

The simulation results thus obtained are shown in Fig. 7 and Fig. 8. Fig. 7(a) shows that the force is controlled in the encircled region. Though at the instant of first impact the interaction force generated is of very large value, it is controlled to the specified value of limiting force (F_{Lim}) equal to 30N subsequently. The reason for the large value
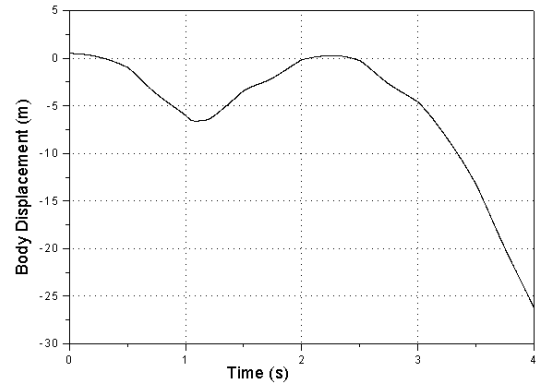
(a)
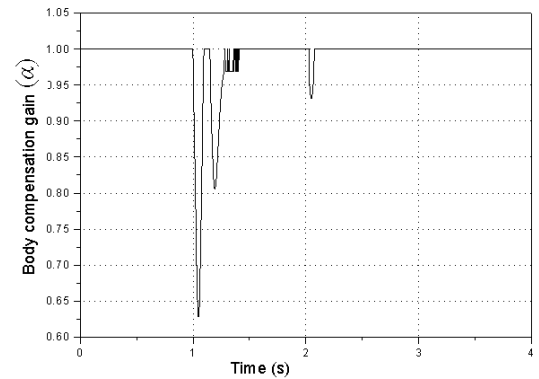
(b)

Fig. 8(a) Body vertical displacement (b) Body compensation gain (α)

of interaction force between the robot toe and the ground i.e. ground impact force (GIF) is the high value of toe velocity at the moment of impact. It can be noted that force is not generated from third cycle onwards due to precise trajectory tracking by the robot toe. In fig. 7(b) it is evident that the robot toe follows the reference trajectory very closely. It is interesting to note that the hopping robot is hopping to a constant height continuously for several cycles. Fig. 8(a) shows that the body experiences considerable displacement in the vertical direction due to the interaction forces generated. This behavior is observed because the hopping robot system is an under-actuated system with two degrees of freedom and only one actuator is used to control the leg. The present modeling does not consider the limits on the body motion. If limiters are designed and modeled then this movement is expected to be within limit value. Fig. 8(b) presents the variation of body compensation gain (α) with respect to time. It varies in

order to accommodate the interaction forces generated between the robot toe and ground as shown in Fig. 7(a).

5 Conclusions

In this paper, impedance control strategy has been used for controlling the impact forces generated during landing phase of the hopping cycle for a one-legged robot. Using this strategy the forces generated during landing has been limited to a constant value specified to the impedance controller. This model and corresponding analysis can be further extended for developing hopping robot response for forward running at different velocities.

References

[1] M. H. Raibert, M.A. Chepponis, and H. Brown: "Experiments in Balance with 3D One-Legged Hopping Machine", *International Journal of Robotics Research*, Vol. 3, pp. 75-92, 1984.

[2] S. H. Hyon and T. Mita, "Development of a Biologically Inspired Hopping Robot- 'Kenken'," *Proceedings of ICRA'02, IEEE International Conference on Robotics and Automation, Washington, DC, pp. 3984-3991, 2002.*

[3] Y. Sato, E. Ohashi and, K. Ohnishi, "Impact Force Reduction for Hopping Robot", *Proceedings of IEEE 31st Annual Conference of IECON'2005, 6-10 Nov. 2005*.

[4] N. Fujii; K. Ohnishi, "Smooth Transition Method from Compliance Control to Position Control for One Legged Hopping Robot", *Proceedings of IEEE International Conference on Industrial Technology, ICIT 2006, pp. 164-169, 15-17 Dec. 2006.*

[5] P. M. Pathak, A. Mukherjee, and A. Dasgupta, "Impedance Control of Space Robots using Passive Degrees of Freedom in Controller Domain", *ASME Journal of Dynamic Systems, Measurement and Control*, 127, 2005, pp. 564-578.

[6] A. Mukherjee, R. Karmarkar and A. K. Samantaray, *Bondgraph in modeling simulation and fault identification*, I.K.International Publishing House Pvt. Ltd., 2006.

[7] A. Mukherjee, *Users Manual of SYMBOLS Shakti*, http://www.htcinfo.com/, High-Tech Consultants, S.T.E.P., Indian Institute of Technology, Kharagpur, 2006.

[8] V. Damic and J. Montgomery, *Mechatronics by bond graphs: An object-oriented approach to Modelling and simulation,* Springer-verlag, 2003.

[9] G. Gilardi and I. Sharf, "Literature Survey of Contact Dynamics Modeling", *Mechanism and Machine Theory* vol. 37, pp.1213-1239, 2002.